Journal of Superconductivity: Incorporating Novel Magnetism, Vol. 17, No. 2, April 2004 (© 2004)

Thermodynamic Properties of the Generalized Falicov–Kimball Model

J. Bonča,[1,2] S. El Shawish,[1] and C. D. Batista[3]

Received 10 August 2003

The thermodynamic properties: specific heat and magnetization are studied as a function of temperature, doping, and interlevel spacing within the two-dimensional extended Falicov–Kimball model for spinless fermions. It was recently shown that the strong coupling limit of the above model possesses electronically driven ferroelectric order. Thermodynamic quantities are calculated using the finite-temperature Lanczos method with additional phase-averaging for a system of 4×4 sites. Our results indicate that valence transition exists in the extended Falicov–Kimball model.

KEY WORDS: Falicov–Kimball model; Hubbard model; valence transition; thermodynamics.

1. INTRODUCTION

The Falicov–Kimball model (FKM) was originally proposed to explain a metal-insulator transition that occurs in transition metals and rare-earth compounds. In its original version [1], the FKM consists of localized f orbitals which interact with a dispersive band of d orbitals through an on-site Coulomb repulsion. A renewed interest in this model started when Portengen *et al.* [2] suggested that introducing hybridization in the FKM might lead to the formation of a new ground state, where d–f excitons Bose–Einstein condense. Such a state possesses macroscopic electric polarization. This suggestion was later supported by the exact solution of the FKM in infinite dimensions [3].

Recently, one of us showed that electronically driven ferroelectricity exists in the strong copling regime of an extended FKM model [4] with no extra hybridization between f and d orbitals. The existence of this new mechanism opens the door to new technological applications because of the strong coupling between the orbital and the spin degrees of freedom of each electron [4]: for instance, a magnetic field can be used as a switch for the ferroelectric state.

The spontaneous ferroelectric (FE) state that exists in the mixed valence regime of the extended FKM is the consequence of a coherent spontaneous hybridization between two atomic orbitals with opposite parity under spatial inversion (f and d in our case) [4]. These state competes with an orbitally ordered (chess board-like) state that is also realized in the mixed valence regime. The most important ingredients necessary for the realization of the electrically polarized state are: (a) the system has to be in the mixed valence regime, (b) the two orbitals which are involved must have opposite parity under spatial inversion, (c) there has to be finite Coulomb repulsion U^{fd} between electrons occupying different bands, (d) unlike in the original FKM, it is best if both bands have a comparable bandwidth, and (e) hybridization between bands is not necessary.

For simplicity, we will consider an extended FKM for spinless fermions. Although the spin degrees of freedom can play an important role because of the coupling with the orbital flavor [4], the philosophy of the present work is to isolate the orbital degrees of freedom, which are responsible for the ferroelectricity, in order to simplify the study of its

[1]J. Stefan Institute, SI-1000 Ljubljana, Slovenia.
[2]Faculty of Mathematics and Physics, University of Ljubljana, SI-1000 Ljubljana, Slovenia.
[3]Theoretical Division, Los Alamos National Laboratory, Los Alamos, 87545 New Mexico.

thermodynamic properties. The Hamiltonian defined on a square lattice is given by:

$$H = \epsilon_d \sum_{\mathbf{i}} n_{\mathbf{i}}^d + \epsilon_f \sum_{\mathbf{i}} n_{\mathbf{i}}^f - t_d \sum_{\langle \mathbf{ij} \rangle} d_{\mathbf{i}}^\dagger d_{\mathbf{j}} + U^{fd} \sum_{\mathbf{i}} n_{\mathbf{i}}^d n_{\mathbf{i}}^f + t_f \sum_{\langle \mathbf{ij} \rangle} f_{\mathbf{i}}^\dagger f_{\mathbf{j}}, \quad (1)$$

where $n_{\mathbf{i}}^f = f_{\mathbf{i}}^\dagger f_{\mathbf{i}}$ and $n_{\mathbf{i}}^d = d_{\mathbf{i}}^\dagger d_{\mathbf{i}}$ are the $f-$ and the $d-$ orbital occupation numbers on the site $\mathbf{i}$. The sum $\langle \mathbf{ij} \rangle$ runs over pairs of nearest neighbor sites. For historical reasons we have named the orbitals as d and f but these two labels can represent any pair of orbitals with opposite parity under a spatial inversion.

While the original FKM can be viewed as a single-particle problem at zero temperature, this is not the case for the extended model given by Eq. (1). This extended model can be exactly mapped into an asymmetric Hubbard model (AHM) [4]. After this mapping, the orbital flavor is replaced by a pseudo spin variable: $c_{\mathbf{i}\uparrow} = f_{\mathbf{i}}$ and $c_{\mathbf{i}\downarrow} = d_{\mathbf{i}}$. Replacing these expressions in Eq. (1), we get the desired expression for H:

$$H = \epsilon \sum_{\mathbf{i},\sigma} n_{\mathbf{i}\sigma} - \sum_{\langle \mathbf{ij} \rangle,\sigma} t_\sigma (c_{\mathbf{i}\sigma}^\dagger c_{\mathbf{j}\sigma} + c_{\mathbf{j}\sigma}^\dagger c_{\mathbf{i}\sigma}) + U^{fd} \sum_{\mathbf{i}} n_{\mathbf{i}\uparrow} n_{\mathbf{i}\downarrow} + B_z \sum_{\mathbf{i}} \tau_{\mathbf{i}}^z, \quad (2)$$

where $\epsilon = (\epsilon_d + \epsilon_f)/2$ and $B_z = \epsilon_f - \epsilon_d$ and $\tau_{\mathbf{i}}^z = (n_{\mathbf{i}}^f - n_{\mathbf{i}}^d)/2$. Without any loss of generality we set $\epsilon = 0$ since a finite ϵ merely represents a shift of the chemical potential. When the original bands have the same dispersion, i.e., $t_f = t_d = t_\sigma$, H is reduced to the original Hubbard model with additional Zeeman coupling to an external magnetic field. For the general case, the SU (2) symmetry of the original Hubbard model is reduced to a U (1) symmetry because of the presence of the Zeeman term and the different hopping amplitudes for each spin polarization ($t_\uparrow \neq t_\downarrow$). It is also important to note that in the new version of our original model, the z-component of the total magnetization couples to the difference between the populations of both bands. Therefore, in the new language the valence instabilities are described as metamagnetic or spin-flop (finite jump in the magnetization) transitions. In a real system, the value of B_z is varied by applying pressure or by alloying. In addition, the orbitally ordered state (chess-board-like) and the Bose-Einstein condensation of excitons are represented by longitudinal (along to the z-axis) and transverse (xy-like) spin density waves, respectively [4].

In our finite temperature study we will focus on the investigation of the thermodynamic properties of the AHM (Eq. (2)) as a function of temperature, doping, and external magnetic field. Our primary objective is to gain deeper physical understanding of the AHM by studying its thermodynamic properties. The motivation of such investigation is primarily coming from the recently established electronically driven spontaneous polarization [4]. Secondly, we want to study how the valence instabilities are affected by the inclusion of a realistic hopping integral for the lower band.

2. METHOD

We study numerically the AHM on a square lattice using the finite temperature Lanczos method (FTLM) [5,6] with the additional phase averaging explained in detail in Refs. [7,8]. In short, the method is based on the Lanczos procedure of exact diagonalization with a random sampling over initial wave functions and phases representing the effect of a uniform vector potential [7,8]. The main limitation to the validity of the results comes from finite size effects which appear at $T < T_{\rm fs}$. The $T_{\rm fs}$ strongly depends on the physical properties of the system. For gapless systems, a criterion for $T_{\rm fs}$ defined through the thermodynamic sum $\bar{Z}(T) = \mathrm{Tr}\ \exp(-(H - E_0)/T)$ calculated in a given system at fixed particle number N_e can be used together with the requirement $\bar{Z}(T_{\rm fs}) = Z^* \gg 1$ [6]. If there is a gap in the excitation spectrum, as is the case for $t_\uparrow \neq t_\downarrow$, this criterion can be relaxed ($Z^* \gtrsim 1$) leading to substantially lower $T_{\rm fs}$.

The calculation of the thermodynamic properties for the original FKM ($t_\uparrow = 0$) does not require to solve a many-body problem [9–12]. Instead, we have to consider all single-particle energies of spin-down electrons moving in a fixed potential created by spin-up particles. The thermodynamic properties are obtained by summation over all possible configurations of spin-up electrons using a grand canonical ensemble and phase-averaging on small square clusters with L sites ($L = 16$). In this way the finite size effects are considerably suppressed in general and more specifically for the largest dopings $n \sim 0.6$–0.8.

3. RESULTS

3.1. Specific Heat and Magnetization at Zero B_z

Using FTLM with additional phase averaging on 4×4 lattice for $t_\uparrow/t_\downarrow \neq 0$ and sampling over all possible noninteracting states for the case of $t_\uparrow = 0$ we evaluate the entropy density s:

$$s = \ln \Omega/N + (\langle H\rangle - \mu\langle N_e\rangle)/NT, \qquad (3)$$

where N_e is the total electron number operator, connected to electron density through $n = n_\uparrow + n_\downarrow = \langle N_e\rangle/N$. From s we obtain the specific heat $C_V = T(\partial s/\partial T)_\mu$.

In Fig. 1 we present $C_V(T)$ for $U^{\rm fd} = 8$, different ratios of $t_\uparrow/t_\downarrow$ =1.0,0.3,0.1,0.0, and $B_z = 0$. We first comment on results calculated at half filling, i.e., $n = 1$. The case $t_\uparrow/t_\downarrow = 1$ corresponds to the original SU (2) invariant Hubbard model. The low energy peak at $n = 1$ is associated with spin excitations. In terms of our original model, these spin excitations represent the Goldstone modes of the orbital ordering and the Bose-Einstein condensation of excitons which

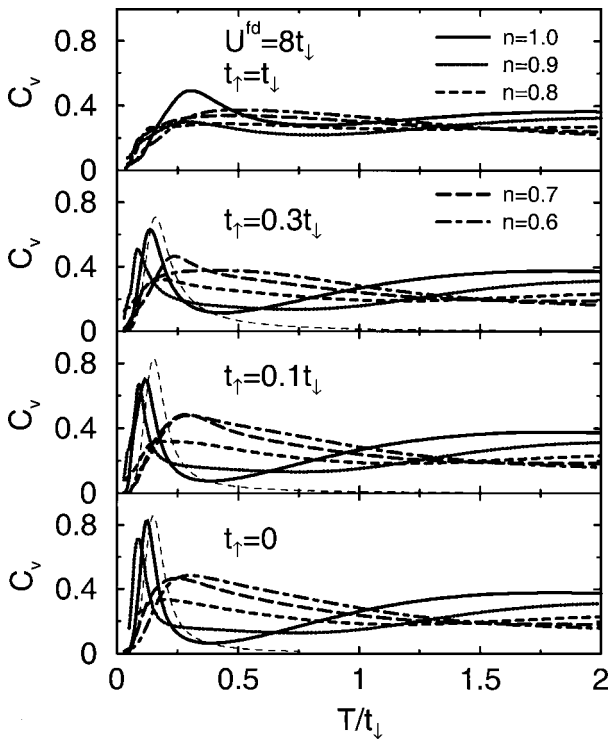

Fig. 1. Specific heat C_V (per unit cell) versus T for $U^{\rm fd} = 8$, $B_z = 0$, various electron densities n and different ratios of $t_\uparrow/t_\downarrow$. Tiny dashed lines represent C_V for the $S = 1/2$ XXZ model (see also the text).

are degenerate at the SU (2) invariant point. In the large $U^{\rm fd}$ limit, $U^{\rm fd} > W = 4(t_\uparrow + t_\downarrow)$, this peak is at $t_\uparrow = t_\downarrow$ approximately located at $T = 8t_\downarrow^2/3U^{\rm fd}$ [7,13]. In this limit, the low energy physics of the Hubbard model for $n = 1$ can be mapped into a Heisenberg model. The broad high-energy peak located around $T \sim U^{\rm fd}/4.8$ is associated with charge excitations [13]. With decreasing the ratio $t_\uparrow/t_\downarrow$, the low-energy peak becomes substantially sharper and moves towards lower temperatures. At $t_\uparrow = 0$, i.e., for the original version of the FKM, our calculations qualitatively agree with the results of Farkašovský [11].

The low temperature behavior of C_V at $n = 1$ is easy to understand if we take into consideration that the low energy spectrum of the AHM maps into an $S = 1/2$ XXZ model in the strong coupling regime. The effective couplings are: $J_z = 2(t_\uparrow^2 + t_\downarrow^2)/U^{\rm fd}$ and $J_\perp = 4t_\uparrow t_\downarrow/U^{\rm fd}$ [4]. The $C_V(T)$ curves calculated with XXZ model on a 20 lattice sites are presented in Fig. 1 with tiny dashed lines for $t_\uparrow/t_\downarrow = 0.3$, 0.1, 0. The peak positions and the widths are well captured by this effective model even though the ratio $U^{\rm fd}/W$ is not so high. The XXZ model becomes an Ising model when $J_\perp = 0$. If we consider that the Ising variables take the values ± 1, the effective coupling becomes $J_{\rm Ising} = J_z/4 = t_\downarrow^2/2U^{\rm fd}$. The C_V of the Ising model has a logarithmic singularity at the phase transition temperature $T_c \sim 2.27 J_{\rm Ising} \sim 1.14/U^{\rm fd}$ which roughly agrees with the position of the low temperature peak at $t_\uparrow = 0$. Because of obvious limitations in the size of our system we can not study the development of the singularity in the specific heat that is expected for the thermodynamic limit. Instead of this singularity, we observe a finite peak which becomes sharper for lower values of $t_\uparrow/t_\downarrow$, since the effective model becomes more Ising-like.

There is a substantial difference in C_V between the symmetric and the AHM models at low temperatures. In the symmetric case, the low temperature behavior is governed by the two-dimensional magnon spectra which leads to $C_V \propto T^2$, while for $t_\uparrow/t_\downarrow \neq 1$ a gap opens in the magnon spectrum leading to an exponentially activated behavior of C_V. Those details can not be clearly seen in Fig. 1 because we are unable to study the system at low enough temperatures.

At small doping away from half-filling, e.g., $n = 0.9$, the low temperature peak at $t_\uparrow/t_\downarrow = 1$ substantially diminishes, while for $t_\uparrow/t_\downarrow < 1$ it moves toward smaller temperatures indicating a softening of the low energy collective excitations. At even larger dopings, e.g., $n \lesssim 0.7$, the two peaked structure completely disappears. In the symmetric limit, C_V approaches the

result for noninteracting electrons, while for $t_\uparrow/t_\downarrow \neq 1$ an asymmetric peak at $T/t_\downarrow \sim 0.25$ develops in the specific heat and at even lower temperatures exponentially approaches zero. This rather unexpected difference is caused by the fact that doping away from half-filling turns the asymmetric system into a band ferromagnet where ferromagnetism is in addition driven by the strong Coulomb repulsion $U^{\rm fd}$.

A more detailed understanding of the behavior of our model for various band fillings can be gained by inspecting the magnetization $M = (n_\uparrow - n_\downarrow)/2$ as a function of filling n which is presented in Fig. 2. M is zero for any filling in the symmetric limit. In contrast, a finite magnetization is obtained by doping away from half-filling the asymmetric system ($t_\uparrow \neq t_\downarrow$). As the band filling decreases, a larger number of spin-up electrons is removed from the system because of highier density of states of the spin-up polarization band at the Fermi level. The effect of the interaction at smaller fillings $n < 1$ is to increase the magnetization in comparison to its noninteracting value. For $U^{\rm fd} = 0$, the magnetization peaks at $n^* = 0.5$ with a maximum value of $M(n = 1/2, T = 0) = n/2 = 0.25$. At finite $U^{\rm fd}$, for all the interacting cases presented in Fig. 2, the peak value $M(n^*)$ exceeds the noninteracting limit. If $t_\uparrow = 0$, $M(n)$ nearly follows its saturated value $M = n/2$, presented with a tiny dashed line, in the interval $0.6 \lesssim n \lesssim 0.7$. Therefore, even though ferromagnetism in the AHM at $n < 1$ is a band effect, finite Coulomb repulsion $U^{\rm fd}$ enhances the magnetization. This is an expected behavior, since by transferring charge from the band with lower occupancy to the more populated one the interband Coulomb energy is reduced.

3.2. Thermodynamics at Finite B_z

In this subsection we focus on the thermodynamic properties at half-filling, $n = 1$, as a function of the pseudomagnetic field $B_z = \epsilon_f - \epsilon_d$, which in the original version of the extended FKM (Eq.(1)) represents the energy difference between the centers of the f and d bands. Starting with $C_V(T)$, shown in Fig. 3, we first notice that the effect of B_z on the low-T behavior of $C_V(T)$ changes substantially between the symmetric and the asymmetric limits. While the effect of increasing B_z is small for $t_\uparrow = t_\downarrow$, a much more pronounced change is observed in the asymmetric case. In particular, increasing B_z for the symmetric case in the interval $0 \leq B_z < t_\downarrow$ only diminishes slightly the low-T peak. In contrast, if $t_\uparrow = 0.3t_\downarrow$ the

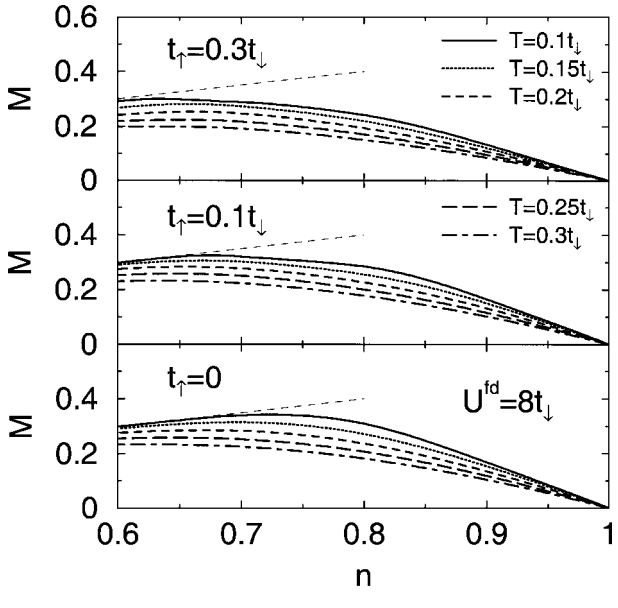

Fig. 2. Magnetization M (per unit cell) versus n for $U^{\rm fd} = 8$, $B_z = 0$, various temperatures T and different ratios of $t_\uparrow < t_\downarrow$. Tiny dashed lines represent $T = 0$ and $U^{\rm fd} = 0$ saturation limit $M = n/2$.

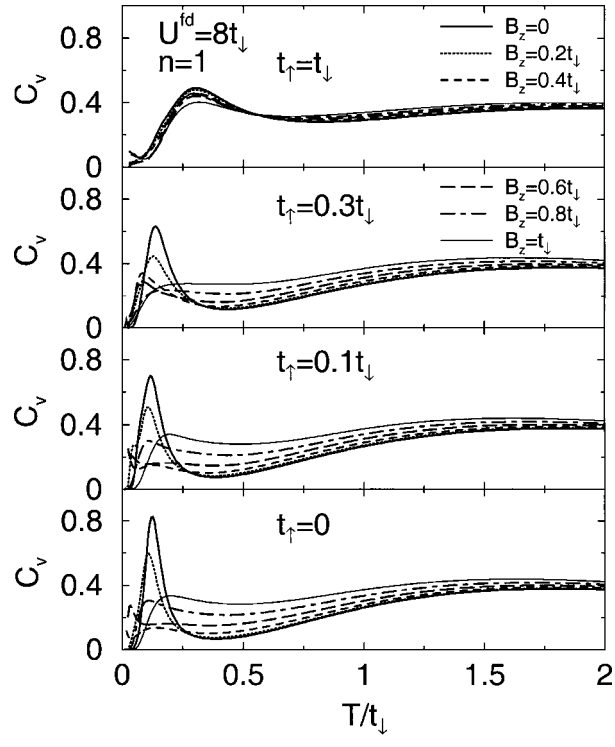

Fig. 3. Specific heat C_V (per unit cell) versus T for $U^{\rm fd} = 8$, $n = 1$, various values of B_z and different ratios of $t_\uparrow/t_\downarrow$.

low-T peak moves toward smaller temperatures and broadens in the regime $B_z \lesssim 0.8t_\downarrow$. For $B_z \gtrsim 0.8t_\downarrow$ only a broad shoulder remains visible. For an even smaller ratio of the hoppings, $t_\uparrow = 0.1t_\downarrow$,0, and $Bz \gtrsim 0.4t_\downarrow$, the low-$T$ peak either completely disappears or moves to temperatures which are not accessible to our calculations. $C_V(T)$ is small and nearly T- independent at low temperatures, $0.05 < T/t_\downarrow < 0.5$, in the interval $0.4 < B_z/t_\downarrow < 0.6$. Such a behavior indicates that the entropy increases at low-T. As we can see in Fig. 4, the magnetization changes very rapidly in this interval of magnetic fields. For larger values of the magnetic field, $B_z \gtrsim 0.8_\downarrow$, the low-$T$ behavior of $C_V(T)$ shows again the activated behavior of a gaped systems. In terms of the original language, this is the band gap originated by the complete transfer of charge from the d to f band. In terms of the spin variables, the magnetization is saturated ($M = n/2$) and there is an energy gap proportional to $|B_z - B_z^c|$ (B_z^c is the critical field that saturates the magnetization) [4].

In Fig. 4, we also show M (T, B_z) for different values of asymmetry ratio $t_\uparrow/t_\downarrow$ and $n = 1$. Note that for $B_z = 0$, $M(T) = 0$ in all the cases. While at high temperature, i.e., $T/T_\downarrow > 1$, $M(T, B_z)$ shows a small variance between systems with different values of $t_\uparrow/t_\downarrow$, the change is much more pronounced at small temperatures. In the symmetric limit, $M(T, B_z)$ changes nearly linearly with increasing B_z. Away from this limit, a strong nonlinear behavior resembling a meta magnetic transition is observed at low temperatures for $t_\uparrow/t_\downarrow \sim 0.3$. This behavior is more pronounced near $t_\uparrow \sim 0$. A meta magnetic transition in the AHM model corresponds to a valence transition in the extended FKM. Because of our limitation to small system sizes that is reflected in our inability to extend the calculation to smaller temperatures, we are unable to determine weather the jump in $M(T \to 0, B_z)$ is discontinuous for $t_\uparrow < t_\downarrow$ or is just a rapid crossover. Quantum Monte Carlo simulations of the XXZ model [14] in very large clusters show that there is a discontinuous change of the magnetization as a function of B_z. This is then the expected behavior for the strong coupling limit of our AHM.

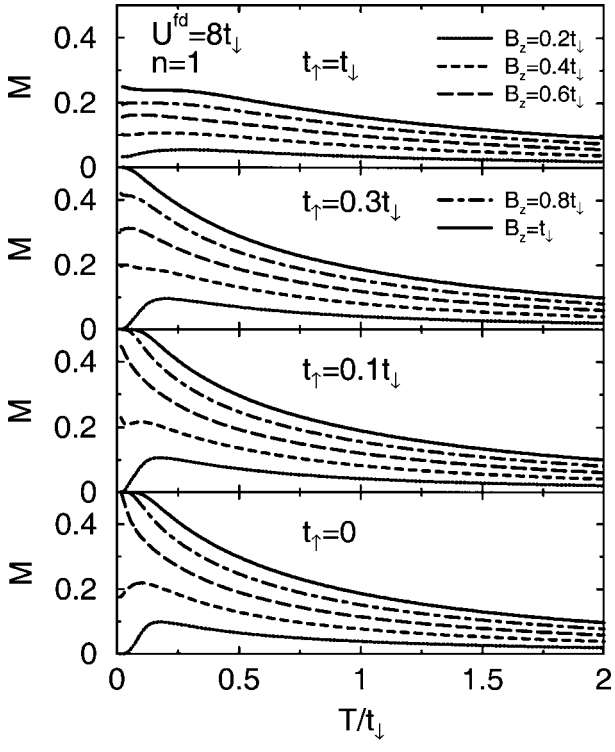

Fig. 4. Magnetization M (per unit cell) versus T for $U^{\mathrm{fd}} = 8, n = 1$, various values of B_z and different ratios of $t_\uparrow/t_\downarrow$.

4. CONCLUSIONS

We have studied the thermodynamic properties of the AHM as a function of T, n, and B_z. In particular, we followed the change of the thermodynamic properties as the system evolves from its symmetric limit represented by the original Hubbard model ($t_\uparrow = t_\downarrow$) to the other limiting case, $t_\downarrow = 0$, which corresponds to the original FKM for spinless fermions. The results of $C_V(T)$ for $n = 1$ and $B_z = 0$ always show two peaks: a low-T peak associated with low energy collective spin excitations (orbital excitations in the original language) and a high energy peak that corresponds to charge excitations. More pronounced differences between the symmetric and asymmetric regimes appear in the specific heat away from half-filling. This effect is related to the band ferromagnetism produced by the different hopping amplitudes of each spin polarization which, in addition, is enhanced by the presence of a strong Coulomb interaction. The enhancement of ferromagnetism by U^{fd} is clearly seen in the $M(n)$ plots where the saturation value of the magnetization ($M = n/2$) is reached in a wide interval of densities and temperatures.

The response of the system to the external magnetic field B_z or the shift of the f level position in the original FKM strongly depends on the ratio of $t_\uparrow/t_\downarrow$ as well. In the symmetric limit only small changes are seen in C_V as B_z is varied in the interval $0 < B_z/t_\downarrow < 1$. In the asymmetric case, B_z is much more effective in softening and suppressing collective spin excitations

causing the shift and suppression of the low-T peak of C_V, which is accompanied by the rapid change of the magnetization with increasing B_z. Rapid change in magnetization represents a valence transition driven by the shift of the f level position in the original FKM. Our results indicate that this valence transition exists in the extended FKM for the whole range of hopping ratios $t_\uparrow < t_\downarrow$ and disappears when this ratio becomes equal to one.

REFERENCES

1. L. M. Falicov and J. C. Kimball, *Phys. Rev. Lett.* **22,** 997 (1969).
2. T. Portengen, Th. Östreich, and L. J. Sham, *Phys. Rev. Lett.* **76,** 3384 (1996); T. Portengen, Th. Östreich, and L. J. Sham, *Phys. Rev. B* **54,** 17452 (1996).
3. V. Zlatić, J. K. Freericks, R. Lemanski, and G. Czycholl, *Philos. Mag. B* **81,** 1443 (2001).
4. C. D. Batista, *Phys. Rev. Lett.* **89,** 166403 (2002).
5. J. Jaklič and P. Prelovšek, *Phys. Rev. Lett.* **77,** 892 (1996).
6. J. Jaklič and P. Prelovšek, *Adv. Phys.* **49,** 1 (2000).
7. J. Bonča and P. Prelovšek, *Phys. Rev. B* **67,** 085103 (2003).
8. D. Poilblanc, *Phys. Rev. B* **44,** 9562 (1991).
9. J. K. Freericks and V. Zlatić, *Phys. Rev. B* **58,** 322 (1998).
10. J. K. Freericks, *Phys. Rev. B* **47,** 9263 (1993).
11. P. Farkašovský, *Z. Phys. B* **102,** 91 (1997).
12. C. A. Macêdo, L. G. Azevedo, and A. M. C. Souza, *Phys. Rev. B* **64,** 184441 (2001).
13. T. Paiva, R. T. Scalettar, C. Huscroft, and A. K. McMahan, *Phys. Rev. B* **63,** 125116 (2001).
14. G. Schmid, S. Todo, M. Troyer, and A. Dorneich, *Phys. Rev. Lett.* **88,** 167208-1 (2002).